Carbohydrate Research 483 (2019) 107753

Contents lists available at ScienceDirect

Carbohydrate Research

journal homepage: www.elsevier.com/locate/carres

Changes in the composition and structure of cell wall polysaccharides from *Artemisia annua* in response to salt stress

Marília Locatelli Corrêa-Ferreira[a], Eliane Batista Viudes[b], Pedro Melillo de Magalhães[c], Arquimedes Paixão de Santana Filho[a], Guilherme Lanzi Sassaki[a], Ana Cláudia Pacheco[b], Carmen Lúcia de Oliveira Petkowicz[a,*]

[a] Department of Biochemistry and Molecular Biology, Federal University of Parana, PO Box 19046, 81531-980, Curitiba, Parana, Brazil
[b] Oeste Paulista University, Rod. Raposo Tavares, Km 572, 19067-175, Presidente Prudente, São Paulo, Brazil
[c] CPQBA, University of Campinas (UNICAMP), Avenida Alexandre Cazellato, 999, 13.140-000 Paulinia, São Paulo, Brazil

ARTICLE INFO

Keywords:
Abiotic stress
Arabinose
Hemicellulose
Pectin
Salinity
Xylan

ABSTRACT

Artemisia annua is cultivated mainly for isolation of artemisinin, a potent antimalarial compound. Moderate salt stress has been proved to increase the artemisinin synthesis by the plant. The aim of this study was to evaluate the influence of salt stress on physiological parameters and cell wall polysaccharides of *A. annua.* Plants subjected to salt stress displayed reduction in the biomass and length and showed high damage of cellular membranes. Cell wall polysaccharides extracted from aerial parts with hot water, EDTA and NaOH also exhibited modifications in the yield and monosaccharide composition. The main changes were found in the pectic polysaccharides: increase of homogalacturonan domain, increase of neutral side chains and increase in the methyl esterification. ^{1}H NMR analyses of pectins indicated that for *A. annua*, arabinans have an important role in coping with salt stress. Hemicellulose domain was also modified under salt stress, with increased xylose contents. The results indicated adaptations in the cell wall of *A. annua* under salt stress.

1. Introduction

Artemisia annua L. (Asteraceae), also known as sweet wormwood, is a medicinal plant, source of artemisinin [1]. In order to supply the demand for the compound, this plant has been widely cultivated in China, Turkey, Vietnam, Afghanistan and Australia [2]. Plant growth and productivity is adversely affected by several abiotic and biotic stress factors, including salt stress, which is the major environmental stress [3]. Natural salinization affects about 1 billion ha and human induced salinization, through irrigation for example, occurs on around 77 million ha [4]. Sodium chloride is the main salt that inhibits cell division and expansion in these saline environments [5].

Although salt stress negatively affects the plant development, it has been demonstrated that moderate salt stress increases artemisinin biosynthesis in *A. annua* [6,7]. Under this condition *A. annua* demonstrated reduction of plant growth and biomass accumulation, oxidative stress, decrease of chlorophyll content and inhibition of nitrate reductase and carbonic anhydrase activities [6,8]. However, salt stress may also affect others aspects of plant development, such the composition and architecture of cell wall [9,10], which has not been evaluated in *A. annua* yet.

The cell wall is a dynamic and complex structure of plant cell, which is fundamental to the plant growth and mediates the interaction between the cell and its environment [11]. Under abiotic stress, the cell wall architecture is modified in order to tolerate the new environmental condition [11]. Changes in the total sugar content, monosaccharide composition and extractability of polysaccharides in response to salt stress have been reported for cell wall of coffee plants [9], grapevines [10] and soya beans [12]. For the seagrass specie *Ruppia maritima*, sulfated polysaccharides were found in response to high salinity. In the absence of salt, sulfated polysaccharides completely disappeared, suggesting that sulfated polysaccharides in plants is an adaptation to high salt environments [13].

Xie et al. [14] reported the presence of sulfate in five polysaccharide fractions isolated from the leaves of *Artemisia tripartita*. However, none of the accepted cell wall models describe the presence of sulfated polysaccharides in terrestrial plants [15,16]. Typically, they are found in marine angiosperms [17] and algae [18]. Thus, we hypothesize that high salinity might trigger the biosynthesis of sulfated polysaccharides in *Artemisia* sp.

* Corresponding author.
E-mail address: clop@ufpr.br (C.L. de Oliveira Petkowicz).

https://doi.org/10.1016/j.carres.2019.107753
Received 12 April 2019; Received in revised form 18 July 2019; Accepted 22 July 2019
Available online 23 July 2019

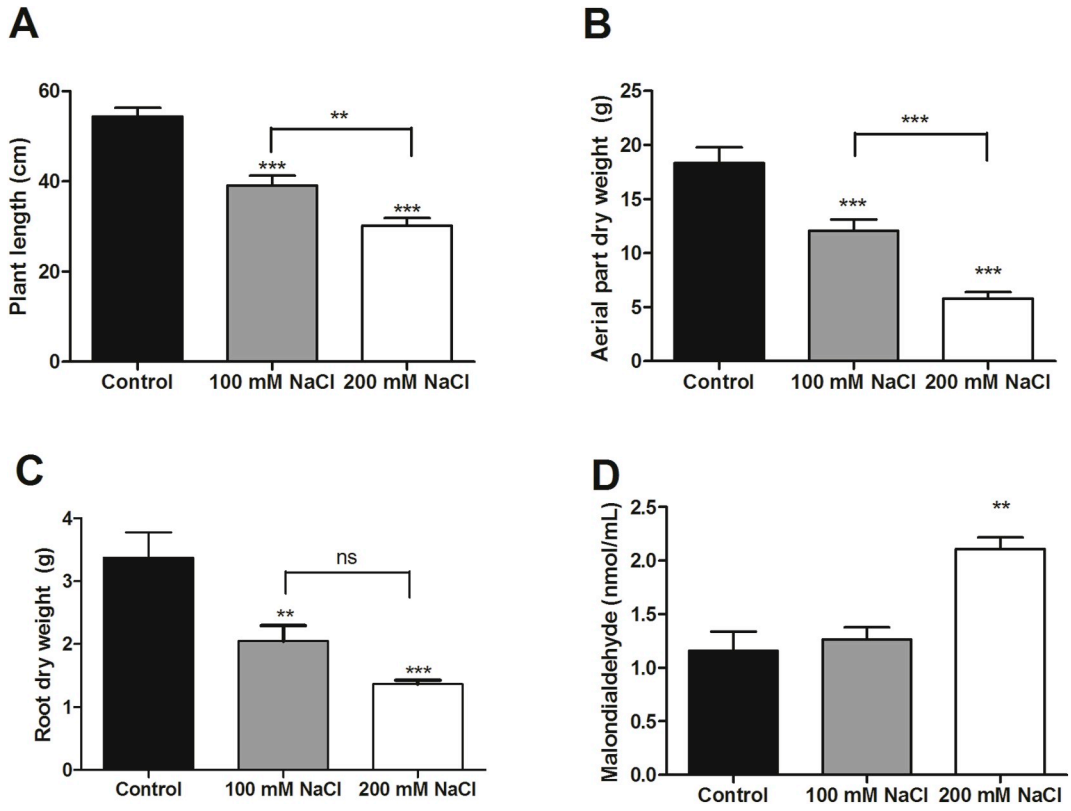

Fig. 1. Effect of salinity on growth and malondialdehyde content in *A. annua* plants. (A) Average length of plants; (B) Aerial parts dry weight; (C) Root dry weight; (D) Leaf malondialdehyde content. Symbols: **P < 0.01, ***P < 0.001, statistically different from control plants. ns: non-significant. Data represent the mean ± standard error (vertical bars) of at least 10 individual plants from each treatment.

Therefore, the aim of the present work was to describe the main changes in the cell wall polysaccharides from aerial parts of *A. annua* grown under salt stress conditions and investigate if sulfation was one of responses to salt stress.

2. Results and discussion

2.1. Effects of salt stress on the physiological parameters of A. annua

Soil salinity is an important factor which hampers crop productivity by altering several aspects of plant physiology [19]. Soil is considered saline, when the electrical conductivity (ECe) is 4 dS/m or more, which is equivalent to approximately 40 mM NaCl [20]. However, plants exhibit different sensibility to salt stress. For *A. annua*, NaCl concentration between 60 and 200 mM has been used in previous experiments [6–8]. In the present study, *A. annua* plants were exposed to a moderate salt stress (100 mM NaCl) and severe stress (200 mM NaCl).

Salt stress negatively affected the growth of *A. annua* plants. After 45 days, average length of plants treated with 100 and 200 mM NaCl decreased by 28.1 and 44.5%, respectively, compared to the control group (Fig. 1A). Similar results were found by Aftab et al. [6]. They observed a reduction of 37.5% in the plant length when submitted to 200 mM NaCl. In the present study, aerial biomass decreased in both treatments, in a dose-dependent manner, displaying a reduction of 37.4 and 65.2%, in 100 and 200 mM NaCl (Fig. 1B). Aftab et al. [6] observed a reduction of 42.6% in the shoot dry weight when *A. annua* plants were submitted to 200 mM NaCl.

Root biomass was also negatively affected by salinity (Fig. 1C). Plants exposed to 100 mM NaCl showed a reduction of 40.0% in root biomass while plants growing in 200 mM NaCl exhibited a reduction of 59.6%. On severe stress (200 mM NaCl), root growth was less affected than shoot growth. Although roots are directly exposed to salt, they are remarkable robust and usually, their growth are less affected than shoots [21].

The marked decrease in the height and biomass of *A. annua* plants under salt stress reflects the toxic effects of NaCl on plant metabolism. Salinity affects the plant development through osmotic stress, which reduces the turgor pressure in the cells, and consequently, it hinders the division and expansion of meristematic cells [11,22]. Besides, the ionic stress caused by saline treatment impairs the production of plant biomass, since the high concentration of total salts causes inactivation of enzymes and protein synthesis [3,23].

The damaging effect of salt stress on *A. annua* plants was also observed by the increase in the malondialdehyde (MDA) levels in the leaves. MDA is a product of lipid peroxidation in cellular membranes and largely used as oxidative stress marker [24]. When plants are submitted to environmental stresses, reactive oxygen species (ROS) accumulate within the cells, generating oxidative damage on cellular structures, such as plasmatic membrane [25]. Severe stress induced an increase of 81.9% in MDA levels (Fig. 1D), indicating high oxidative damage in the cell membranes. This increase in MDA content is in agreement with a previous report which described an increase of 98% of MDA contents in *A. annua* plants subjected to 200 mM NaCl [6]. This result confirms that 200 mM NaCl was able to induced oxidative stress in the aerial parts of *A. annua*.

2.2. Changes in the cell wall composition of aerial parts of A. annua submitted to salt stress

The impact of abiotic stress on cell wall polysaccharides on several crops has been reviewed [11,22]. Salt stress affects the structure and composition of cell wall polysaccharides, but distinct responses are observed when different plant species are compared. However, no information regarding the remodeling of the cell wall polysaccharides

from *A. annua* specie in response to salt stress was found in the literature. In order to gain understanding on this subject, dried aerial parts of *A. annua* plants from control and salt stress conditions were sequentially extracted with hot water (W), 100 mM EDTA (E) and 6 M NaOH, to obtain pectins and hemicelluloses.

In response to high-salinity environment, *Ruppia maritima* (halophytic specie) produces sulfated polysaccharides as an adaptation mechanism to survive in this condition [13]. Although the accepted cell wall models do not describe the presence of sulfated polysaccharides in terrestrial plants [15,16], the presence of sulfate has been reported for polysaccharides from other *Artemisia* species. Polysaccharide fractions obtained by hot-water extraction from leaves of *A. tripartite* were reported to contain at least 3.4% of sulfate and consisted primarily of xylose, glucose, arabinose, galactose, and galactosamine [14]. Sulfate was also reported to be found in purified polysaccharides from stem lettuce (*Lactuca sativa*), from Asteraceae family [26]. Thus, the presence of sulfate in the polysaccharides of *A. annua* (Asteraceae) was also investigated. Colorimetric [27] and turbidimetric [28] assays showed that no polysaccharide fraction from *A. annua* contained sulfate, indicating that *A. annua* did not produce sulfated polysaccharides as reported for *A. tripartita,* neither in response to salt stress, as found for *Ruppia maritima* [13]. Aqueous and EDTA fractions also were evaluated by FT-IR (Fig S5 – S6). The absence of characteristic absorption bands from sulfate groups (800–850 cm^{-1}) on FT-IR spectra confirmed this result.

Instead, changes observed under salt stress were related to the yield and composition of polymers. The amount of pectins extracted with chelating agent (EDTA) decreased significantly compared to control plants (E − 200: 2.5%; E-Control: 5.8%). Changes in the yield of pectic fractions in plants submitted to salt stress was also observed for coffee [9]. For coffee leaves, salt stress was found to decrease the water soluble pectin content but increase the EDTA soluble pectins. On the other hand, in the plant red-osier dogwood the pectin content was not modified under salt stress condition [29]. In the present study, despite the decrease of EDTA soluble pectins, the total pectin content (aqueous and EDTA soluble) was not changed during salt stress, (W + E)-200: 23.2%; (W + E)-Control: 23.8%. The differences in the extractability of polysaccharides under salt stress may reflect the modification in the interaction of the polymers in the cell wall of *A. annua* induced by salt stress [9].

The yield of hemicelluloses and final insoluble residues from aerial parts of *A. annua* (4 month-old plants) were not affected by the salt stress. However, for red-osier seedlings (6 month-old plants) it was observed an increase in the hemicellulose contents in the shoot of salt stressed plants compared to the control. The salt stress may induce alterations in the cell wall polysaccharides indirectly through gene expression, or directly, through physically interaction of Na^+ ions with cell wall components, inducing changes in the cell wall composition. This modifications may vary according to the developmental stage of the cell and also between different plants [30] because the chemical composition of cell wall is modified during the cell development and the strategy used by cells to cope with the salt stress may be different among the species [30,31].

The monosaccharide composition of all fractions obtained from aerial parts of *A. annua* was affected by salt stress. Fractions extracted with water showed high content of uronic acids, arabinose and galactose, suggesting the presence of pectins and arabinogalactans. Fig. 2B exhibits a comparison of monosaccharide composition of aqueous fraction from control and saline treatments. Salinity significantly increased the uronic acids ($P < 0.001$) and reduced rhamnose ($P < 0.05$). Differently, the pectin extracted from the shoot cell walls of red-osier seedlings after treatment with 50 mM NaCl showed reduction in galacturonic acid content and increase of rhamnose [29].

In order to have information about the pectin composition, the ratio between the monosaccharides was calculated. The ratio UA/Rha has been used to estimate the relative abundance of homogalacturonan (HG) versus rhamnogalacturonan-I (RG-I) domains of pectins while the ratio Ara + Gal/Rha has been used to evaluate the relative importance of neutral side chains to the RG-I backbone [32]. The ratio UA/Rha significantly increased in W-100 and W-200 fractions ($P < 0.05$) compared to the control plants, indicating increase of HG domain of pectins from plants submitted to salt stress (Fig. 2C). Increase of carboxylated polysaccharides in the cell wall of plants submitted to high salt environment was also reported for rice (*Oryza sativa*) [13] and coffee plants (*Coffea arabica*) [9]. HG domain has been reported to control of the viscosity and mechanical properties of the cell wall matrix [33] and changes in HG structure may interfere in the plant development [34]. It has been pointed that negatively charged cell wall polysaccharides might increase the Donnan potential, facilitating ion transport from the cell at high salt concentrations and/or slow the movement of Na + toward the cells [35].

On the other hand, a reduction in the levels of uronic acids was found for leaves of grapevines plants under salt stress [10], reinforcing the hypothesis that plants may exhibit different tolerance mechanisms when exposed to saline environments.

Under severe stress, polysaccharides extracted with hot water also showed significant increase in arabinose contents ($P < 0.001$) and in the (Gal + Ara)/Rha ratio ($P < 0.01$), compared to the control plants. These data indicate an increase in neutral side chains of RG-I backbone during salt stress condition. According to the review by Gall et al. [22], the increase in pectin side chains seems to be the only common tolerance mechanism to salt stress shared among plants from different species. Pectins are able to bind water and form gel in the cell wall and the increase of side chains of pectins may protect the cytosol during drought stress. Besides, arabinan-rich pectin would prevent water loss during desiccation [22,36].

W fractions isolated from control and salt treated plants were submitted to a detailed analysis, comparing the ^1H and $^1H/^{13}C$ HSQC NMR spectra. Qualitative analysis of HSQC demonstrated that W-100 and W-200 were very similar to control. Correlations found in the HSQC spectrum of W-Control (Fig. 3A) were also found in the spectra of fractions from salt treated plants. The assignments were based on literature values [37–39]. Due to complexity of the spectra, mainly the anomeric region was analyzed. Chemical shifts typical of homogalacturonan were found in the correlation map. Signals of 1,4-linked unesterified α-D-Gal*p*A were found at δ 99.3/5.11, corresponding to C1/H1 and at δ 68.3/3.74 (C2/H2), 68.9/3.96 (C3/H3), 78.5/4.40 (C4/H4) and 71.7/4.67 (C5/H5). For methyl esterified units, signals at 100.0/4.95 and 100.0/4.92 ppm were assigned to C1/H1 and at δ 78.4/4.45 (C4/H4) and 70.5/5.09 (C5/H5) [40]. Resonance of the methoxy group was observed at δ 52.8/3.81 and those of the acetyl group appeared at δ 20.2/2.09; 20.4/2.15 and 20.5/2.18.

The signals at δ 107.6/5.08 and 107.5/5.10 were assigned to C1 of 1,5 and 1,3,5-linked α-L-Ara*f*. The C5/H5 of Ara (1 → 5) was found at 66.7/3.78/3.81 and for units 1,3,5-linked at 66.7/3.85/3.92. The signals at 76.8/3.95 was attributed to C3/H3 of Ara 1,5-linked and at 81.3/4.12 ppm for 1,3,5-linked Ara. The signal of C3 shifted downfield to 81.3 ppm indicates that this arabinose is also substituted at position O-3 [41].

Signals of anomeric carbon of 1,3-linked and terminal α-L-Ara*f* were found at δ 107.1/5.15 and 109.2/5.25, respectively. These signals indicate the presence of arabinans and/or arabinogalactans as side chains of RG-I. A signal of C1 of β-D-Gal*p* (δ 103.4/4.46) was also found, suggesting the presence of galactans and/or arabinogalactans.

The C6 of 1,2- and 1,2,4-substituted rhamnose were found at δ 16.7/1.24 and 16.8/1.29 ppm, respectively [38], which indicate the presence of RG-I in the aqueous fraction.

The degree of O-methyl esterification of pectins from W fractions of control and saline treatments, determined by FT-IR (Fig. S5), indicated that under salt stress, pectins from *A. annua* were more methyl-esterified (Table 1). Gall et al. [22] suggest that the fine regulation of degree of methyl esterification of pectins and the amount of HG domain in the cell wall determines the stiffness and hydration status of pectic matrix

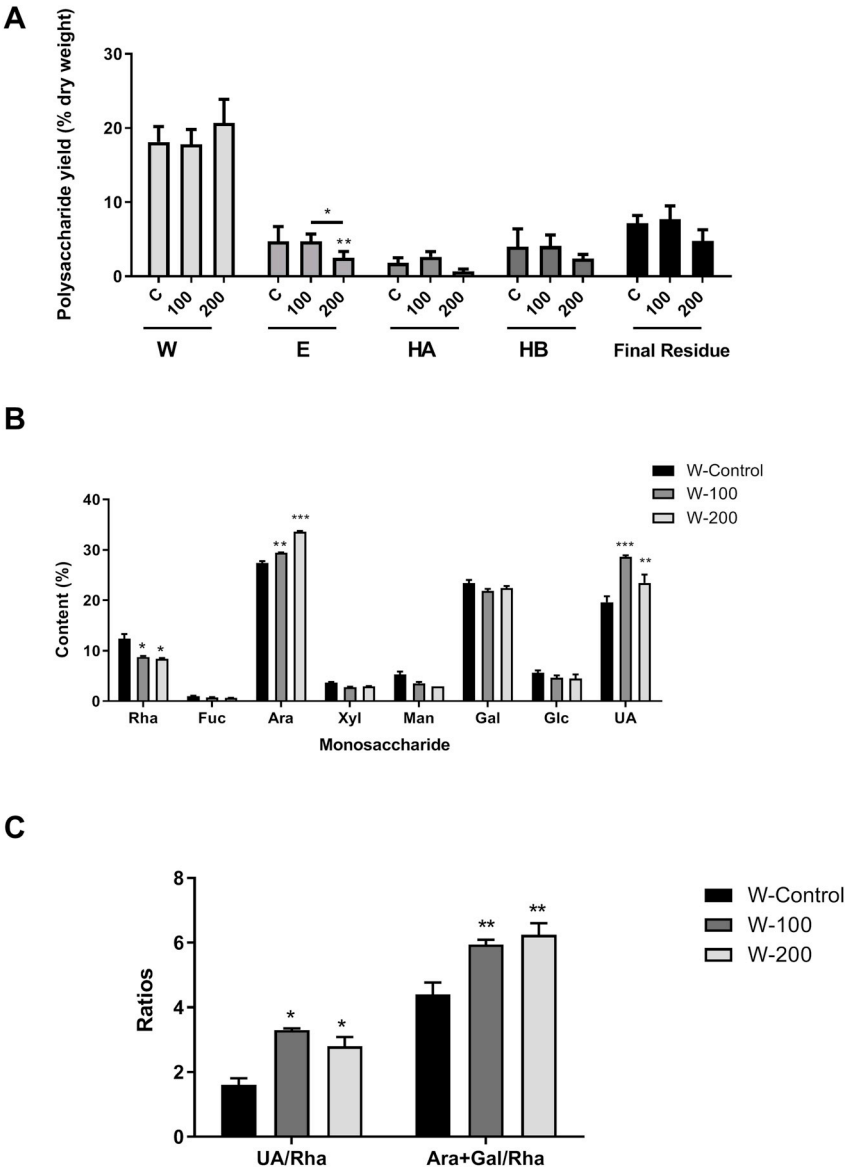

Fig. 2. Effects of salt stress on the yield of fractions extracted from aerial parts of *A. annua* (A); Monosaccharide composition of W fractions (B); UA/Rha and Ara + Gal/Rha ratios (C). Results are expressed as mean ± standard error of the mean of three assays. Symbols: W- fraction obtained with boiling water; E − fraction obtained with 100 mM EDTA; HA - hemicellulose A fraction obtained from 6 M NaOH; HB - hemicellulose B fraction obtained from 6 M NaOH; C – Control plants; 100 - plants submitted to 100 mM NaCl; 200 - plants submitted to 200 mM NaCl. *P < 0.05, **P < 0.01 and ***P < 0.001 statistically different from control plants.

during water deficit. Byrt et al. [30] propose that Na^+ ions may interfere with pectin methylesterases function, thus modifying the degree of methyl esterification of pectins. Different patterns of change in the methyl esterification of pectins when plants are subjected to abiotic stress have been reported. It has been pointed that the discrepancy could be due to different mechanisms of control of pectin methylesterase activity, depending on the genotype, species or tissue [22]. As found for *A. annua*, highly methylated pectin was also observed in petioles of an aspen hybrid plants in response to treatment with 50 mM NaCl [5]. However, a decrease in the degree of methyl esterification in response to 100 mM NaCl was found in the cell wall of leaves from three maize (*Zea mays* L.) hybrids with different salt tolerance. The tolerant hybrid displayed a delayed in the accumulation of non-methylated uronic acids and showed better growth compared to the sensitive one, contributing to salt resistance in the first phase of salt stress [31].

In order to evidence the differences between the samples from control and saline treatments, an integration of signals from ^1H spectrum and principal component analysis (PCA) were performed (Fig. 3B–E).

The signal of acetyl group of pectins from plants submitted to salt stress had higher integral area than that of control plants (Fig. 3B). The role of acetyl in pectins seems to be associated with the cell wall viscosity and prevention of the interaction between pectin and calcium ions [33,42]. In the anomeric region of ^1H spectrum, important changes were observed. Plants submitted to salt stress showed significant increase of integrated area of signals corresponding to arabinose (δ 5.25, 5.15, 5.10, 5.08) (Fig. 3C).

Only the anomeric region was used for PCA analysis. Fig. 3D displays the graph of the scores for PC1 and PC2. The samples from salt treated plants (W-100 and W-200) were clearly distinguished from W-Control by PC1. In the loading plot (Fig. 3E) it was found that the main signals that affect the difference between the treatments are 5.10, 5.08 and 5.15 ppm, which correspond to arabinose residues, confirming the importance of arabinose in the salt stress.

Pectins were also the major components of E fractions as indicated by the predominance of uronic acids, arabinose, galactose and rhamnose. For fractions from salt treatments it was observed an increase of glucose and decrease of uronic acids contents when compared to the control (Fig. 4A). The increase of glucose might indicate an increase in the starch content under salt stress. E−200 and E−100 displayed increased Ara + Gal/Rha ratio (Fig. 4B) indicating higher amount of side chains in the pectin, as also observed for the aqueous fraction.

Analysis of HSQC demonstrated that E−100 and E−200 were very similar to control. Correlations found in the HSQC spectrum of E-

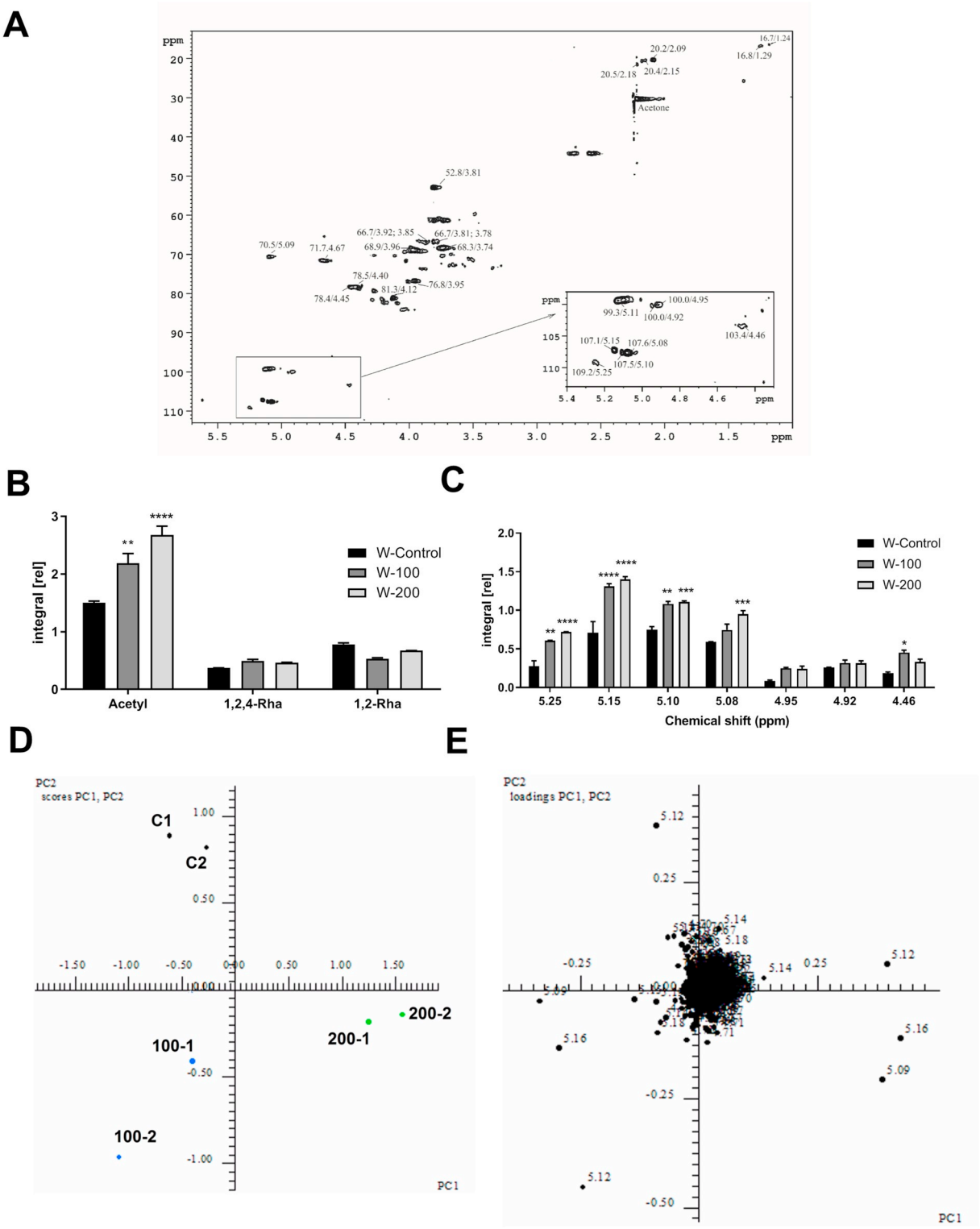

Fig. 3. $^{1}H/^{13}C$ HSQC of W-Control fraction (A); Integrated area of signals from ^{1}H spectrum of W fractions (Acetyl: 2.11, 2.17 ppm; 1,2,4-Rha: 1.29 ppm; 1,2-Rha: 1.24 ppm) (B); Integrated area of signals of anomeric region of ^{1}H spectrum of W fractions. (Chemical shifts: 5.25 – terminal α-L-Ara*f;* 5.15 – 1,3-linked α-L-Ara*f;* 5.10–1,3,5-linked α-L-Ara*f;* 5.08–1,5-linked α-L-Ara*f;* 4.95/4.92 – Gal*p*A methyl esterified; 4.46 - β-D-Gal*p*); (C); Graph of the scores for PC1 and PC2 (D) and Loading plot (E). Symbols: *P < 0.05, **P < 0.01,***P < 0.001 and P < 0.0001 statistically different from control plants. Chemical shifts of $^{1}H/^{13}C$ HSQC are expressed relative to acetone (^{1}H = 2.22 ppm; ^{13}C = 30.2 ppm).

Control are showed at Fig. 5A. It was observed signals of RG-I as evidenced by the signals of C1/H1 of rhamnose at 98.7/5.26 ppm and at *δ* 99.2/5.11 the C1/H1 of unesterified galacturonic acid. Signals of C6 from rhamnose were found at *δ* 16.6/1.25 and 16.9/1.31 ppm [38].

Signal at *δ* 20.3/2.10 was assigned to acetyl groups and at 52.8/3.81 ppm to the methyl group. Arabinan and/or arabinogalactan side chains of RG-I were evidenced by the signals at *δ* 107.6/5.08, 107.6/5.10 and 107.2/5.15 assigned to C1/H1 of α-L-Ara*f* units. Signals of galactose were found at *δ* 104.4/4.61 and 103.7/4.65 corresponding to C1/H1 of 1,4-linked-β-D-Gal*p* units from galactans and/or type I

Table 1
Degree of methyl-esterification of pectins (W and E fractions) extracted from aerial parts of *A. annua*.

Fraction	DE (%)
W-Control	23.5 ± 2.33
W-100	26.2 ± 0.98
W-200	30.8 ± 1.26 *
E-Control	33.7 ± 0.25
E − 100	28.1 ± 1.53
E − 200	25.4 ± 1.98

Values were expressed as mean ± standard error of the mean. Symbols: *P < 0.05 statistically different from control plants.

arabinogalactans (AG-I) and at 103.5/4.42, 102.8/4.49 and 102.8/4.47, corresponding to C1/H1 of 1,3,6-, 1,6- and 1,3-linked-β-D-Gal*p* units from type II arabinogalactans (AG-II). Type II arabinogalactans were also found in the cell wall of aerial parts of *Artemisia absinthium* [43]. Comparing control and saline treatments it was not observed significant differences on the degree of methyl esterification of chelating soluble pectins by FT-IR (Fig. S6), as observed in Table 1. In the $^{1}H/^{13}C$ HSQC, an intense signal at 99.7/5.37 ppm, assigned to the anomeric carbon of α-D-Glc from starch (Fig. 5B), was observed for E − 100 and E − 200, but not in E-Control. These results were confirmed by the significant increase of integrated area of the signal 5.37 ppm in the ^{1}H spectrum of E − 200 compared to E-Control (Fig. 5D; Fig. S3). The increase of starch content in response of salt stress was also observed in potato [44] and tomato [45]. The reduction in the cell division and growth might explain the accumulation of starch in the leaves of plants submitted to salt stress [46].

Comparing the control group, 100 and 200 mM NaCl, no difference were found in the elution profiles from HPSEC analyses using RI detector for fractions W and E (Fig. S1 A-B).

When analyzed by HPSEC using RI detector, W fractions had similar elution profile for all treatments. A slight increase in the relative peak areas of polysaccharides with higher molar mass (37–43 min and 44–48 min) was observed for W-100 and W-200 compared to W-Control (Fig. S1 A), which may be related with the increase of homogalacturonan domain and neutral side chains in the pectins after salt stress. Comparing the EDTA fractions, the elution profiles were very similar for all treatments (Fig S1 B). However, it was observed an increase in the relative peak area between 38 and 45 min for E − 200 compared to E-Control (E-Control ~ 31%; E − 200–40%), suggesting increase of polymers with higher molar mass after salt stress.

Hemicellulose fractions (HA and HB) exhibited xylose as the main monosaccharide, in addition to glucose, mannose, galactose and uronic acids. ^{1}H NMR spectra of hemicellulose fractions (HA-Control and HB-Control) were very similar (Fig. S7). Correlations in $^{1}H/^{13}C$ HSQC indicated the presence of 4-O-methylglucuronoxylan as the main hemicellulose of *A. annua* cell wall. Comparative analyses of HSQC of hemicellulose fractions from control and saline treatments demonstrated similar spectra for all samples. Therefore, only the spectra of HA-Control (Fig. 6A) and HB-Control (Fig. 6B) are shown. Signals at 101.9/4.49–101.7/4.48 ppm were assigned to C1/H1 from 1,4-linked β-D-Xyl*p* and at 76.5/3.78 ppm to C4/H4. Signals at 101.3/4.65–101.2/4.64 ppm were assigned to 2,4-substituted β-D-Xyl*p* and at *δ* 76.9/3.48 and 76.5/3.79 to C2/H2 and C4/H4, respectively. The xylan backbone is substituted in O-2 by 4-O-methyl-α-D-Glc*p*A, as evidenced by the signals at 97.7/5.27–97.6/5.26 ppm of C1/H1 from glucuronic acid, and at 82.4/3.28 ppm from C4/H4 linked. At *δ* 59.8/3.49–59.5/3.47, it was observed signals corresponding to the methyl group. The signal at 23.5/1.92–23.3/1.90 ppm indicates the xylan backbone is acetylated [47]. The correlation at 100.3/4.75–100.0/4.75 ppm may be due to the presence of β-D-Man*p* 1,4-linked, typical of mannans. Signals were assigned based on the HSQC and ^{1}H NMR spectra (Fig. S7) following sugar composition and literature [48–50].

Plants submitted to salt stress had higher levels of xylose than control plants (Fig. 7A and B), indicating an important role of xylose-containing polysaccharides under salt stress. The increase of xylose suggests that under salt stress, the xylan backbone displayed lower degree of substitution. The substitutions along the xylan backbone affect their physicochemical properties, such as the interaction with cellulose in the cell wall [51]. High degrees of substitutions in hemicelluloses restrict the cross-linking with cellulose microfibrils. On the other hand, low degrees of substitution contribute to the stiffening of the cell wall and allow the cell to resist the internal turgor pressure [51,52]. Under salt stress, the tissues of plants loose turgor pressure due to the lower osmotic potential of salinized soil, which induces loss of water by the cells [5]. The increase in the degree of methyl esterification of pectins and the lower degree of substitution in xylan found in *A. annua* under salt stress suggest that the cell wall became more rigid in order to maintain the turgor pressure .

Hemicellulose fractions obtained from aerial parts of *A. annua* displayed polymodal elution profiles by HPSEC (Fig S1 C-D). The main peak of HA fractions from plants submitted to moderate and severe salt stress was shifted to a lower elution time, corresponding to higher molar mass values. An increase in the relative peak area of the polysaccharides eluting between 36 and 46 min was observed for HA-100 and HA-200 compared to HA-Control (HA-Control ~ 6%; HA-100–11%; HA-200–13%).

For HB fractions, the peak eluting around 55 min was shifted to higher molar mass values in the severe stress group compared to the control. However, an opposite trend was observed for the HB fraction extracted from plants subjected to moderate salt stress. No important changes were found among the samples in the relative areas of this peak.

The changes observed by HPSEC along with the increase in the xylose contents found in the monosaccharide composition of *A. annua* plants after the salt stress might indicate the presence of xylans with higher degree of polymerization. Changes in molar mass of polysaccharides after salt stress were also reported for coffee plants [9].

The final insoluble residues of aerial parts from salt stressed plants showed predominance of glucose (70%) and xylose (20%). No

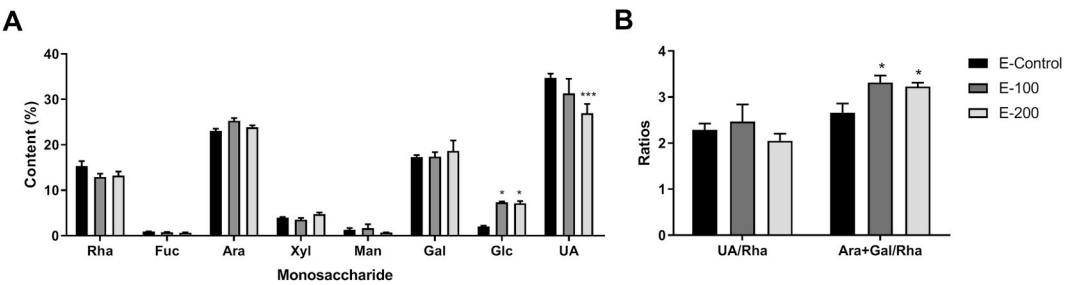

Fig. 4. Effects of salt stress on the monosaccharide composition of E fractions from control and saline treatments (A) and UA/Rha and Ara + Gal/Rha ratios (B). Results are expressed as mean ± standard error of the mean of three assays. *P < 0.05, **P < 0.01 and ***P < 0.001 statistically different from control plants.

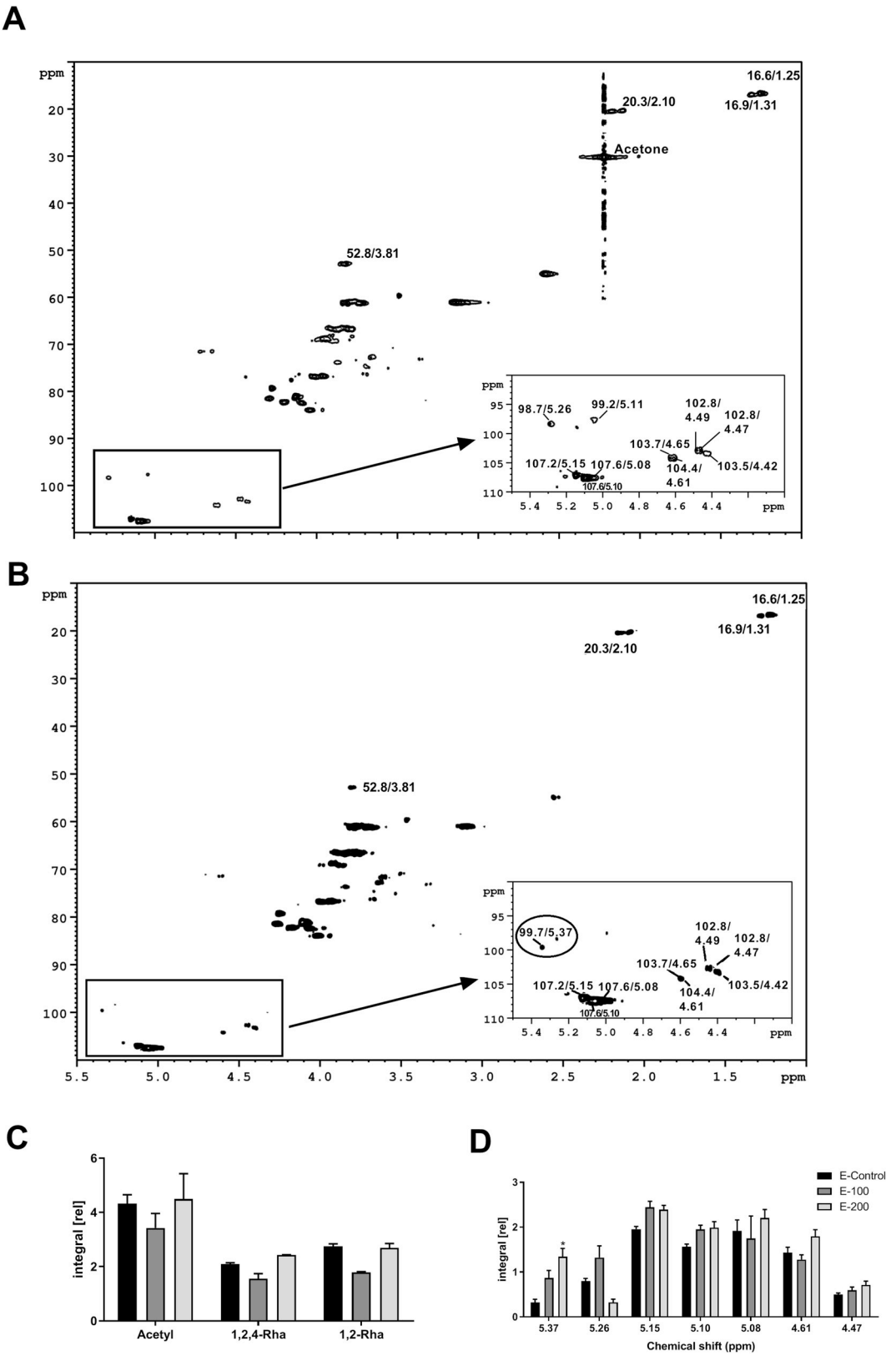

Fig. 5. $^{1}H/^{13}C$ HSQC of E-Control fraction (A). $^{1}H/^{13}C$ HSQC of E − 200 fraction. The circle indicates the signal of glucose from starch. (B) Integrated area of signals from ^{1}H spectrum of E fractions (Acetyl: 2.09, 2.15, 2.18 ppm; 1,2,4-Rha: 1.29 ppm; 1,2-Rha: 1.24 ppm) (C); Integrated area of signals of anomeric region of ^{1}H spectrum of E fractions (Chemical shifts: 5.37 - α-D-Glc, 5.26 – Rha; 5.15 – 1,3-linked α-L-Ara*f;* 5.10–1,3,5-linked α-L-Ara*f;* 5.08–1,5-linked α-L-Ara*f;* 4.61–1,4-linked-β-D-Galp; 4.47–1,3-linked-β-D-Gal*p*). (D). Symbols: *P < 0.05, **P < 0.01 statistically different from control plants. Chemical shifts in $^{1}H/^{13}C$ HSQC are expressed relative to acetone (^{1}H = 2.22 ppm; ^{13}C = 30.2 ppm).

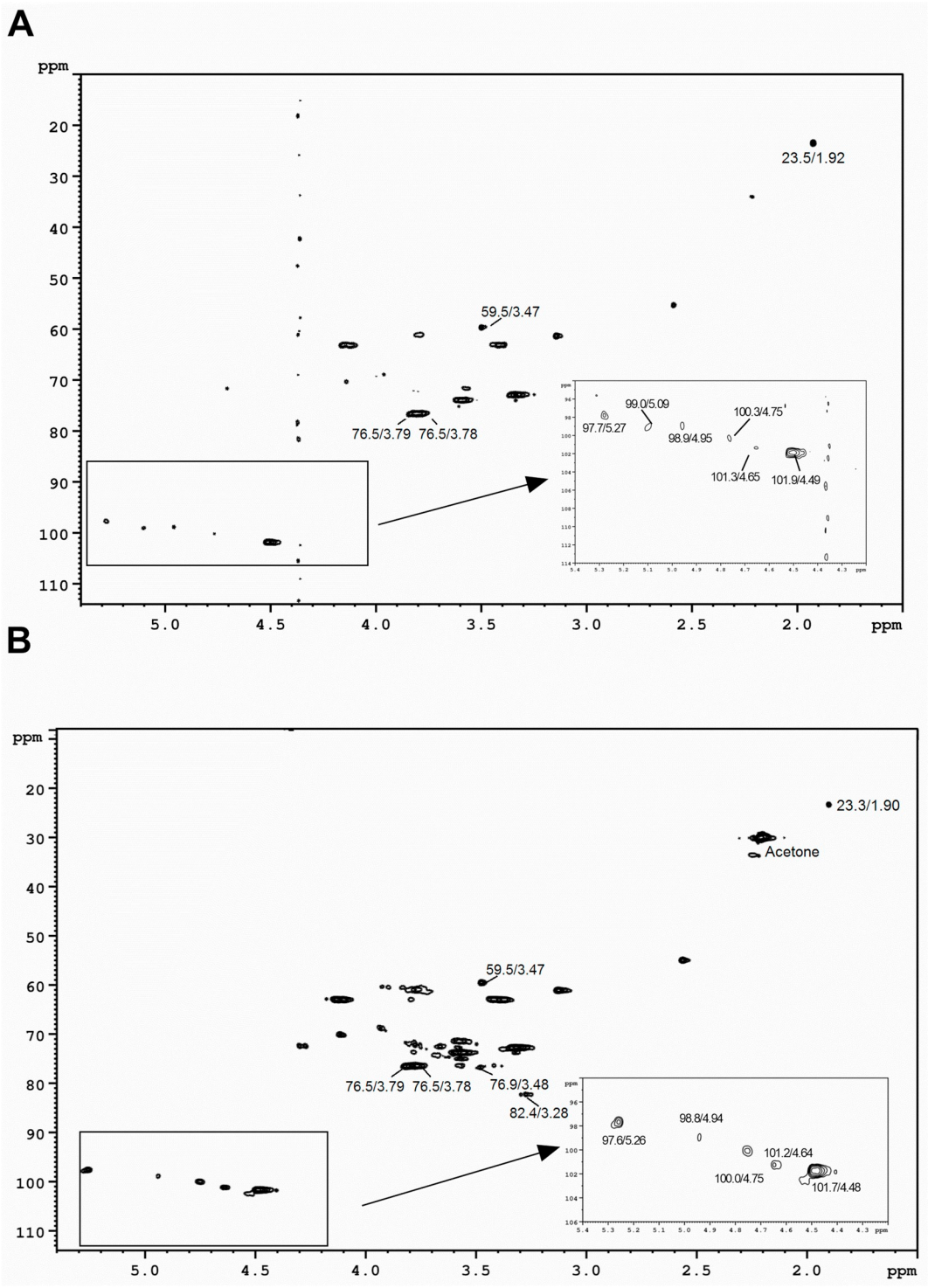

Fig. 6. $^{1}H/^{13}C$ HSQC of HA-Control fraction (A) and HB-Control (B). Sample HA-Control was dissolved in 0.1 M NaOD at 20 mg/mL and spectra were recorded at 70 °C. Chemical shifts are expressed relative to TMPS-*d4* ($\delta = 0$). Sample HB-Control was dissolved in D_2O at 20 mg/mL and spectra were recorded at 70 °C. Chemical shifts are expressed relative to acetone ($^{1}H = 2.22$ ppm; $^{13}C = 30.2$ ppm).

statistical differences were found in the monosaccharide composition between control and salt treated plants.

3. Experimental

3.1. Plant material, growth condition and salinity treatments

Seeds of *A. annua*, provided by Dr. Pedro Melillo de Magalhães from CPQBA (Centro Pluridisciplinar de Pesquisas Químicas, Biológicas e Agrícolas-UNICAMP- SP, Brazil), were sown and after 60 days, the seedlings were transferred to 8 kg pots containing a mixture of Plantmax ® nutrients, soil and sand (1:1:1). The stress experiment was performed in a greenhouse with daily minimum temperatures 17–20 °C and maxima of 26–27 °C, relative humidity 70%. The composition of Plantmax ® is given in Table S1 [53]. Stress conditions were imposed after 15 days of acclimation. Plants were divided in 3 groups: (1)

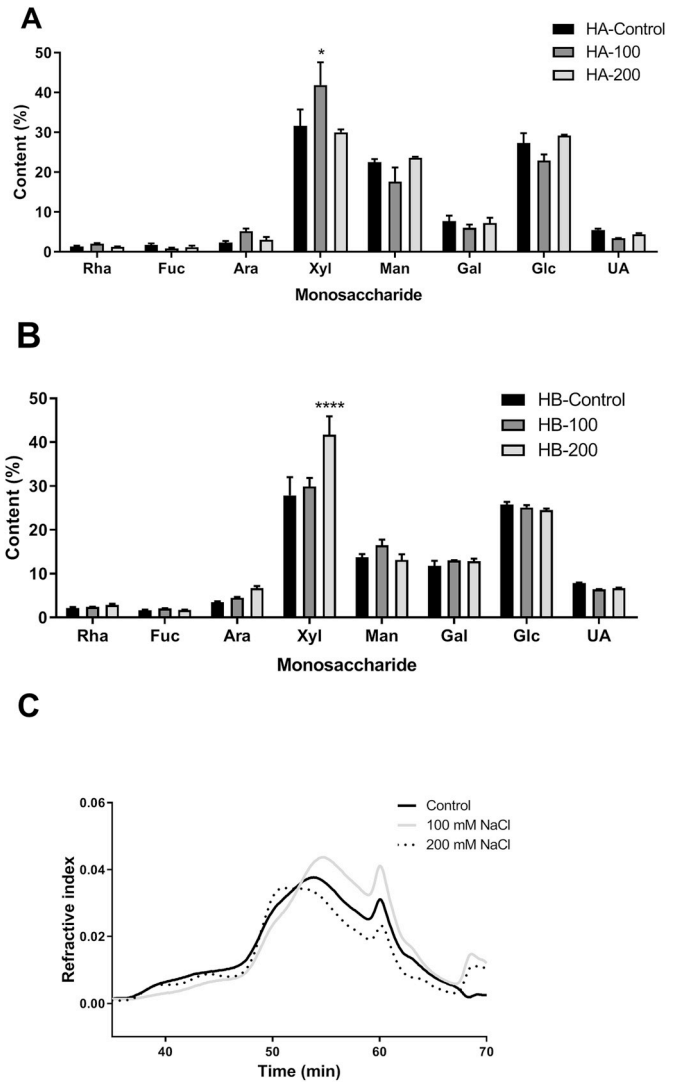

Fig. 7. Effects of salt stress on monosaccharide composition of hemicellulose A fraction from aerial parts (A); and hemicellulose B (B). Values were expressed as mean ± standard error of the mean. Symbols: *P < 0.05 and ****P < 0.0001 statistically different from control plants.

control (0 mM NaCl), (2) 100 mM NaCl, and (3) 200 mM NaCl, with 15 biological replications in each group. The plants received 100 or 200 mM NaCl solutions and the control plants received just water [6]. Plants were watered with solutions 3 times a week until soil saturation, for 45 days. The amount of loss water was determined based on the weight difference with the pots with water saturated substrate [54]. Twenty four hours before harvesting the plants were kept in the dark to deplete starch reserve [55]. After harvesting, plants from each treatment were immediately frozen at −80 °C and then lyophilized. The biometric parameters evaluated were plant length and dry mass of aerial parts and roots. The plant length was measured from the base of the stem (soil level) to the top of the plant. Ten plants per treatment were used.

3.2. Lipid peroxidation rate

The oxidative damage to leaf lipids was evaluated by the trichloroacetic/thiobarbituric acid method [56]. Fresh leaf samples were used in the assay, and the absorbance of samples was measured at 532 and 600 nm. Malondialdehyde equivalents were calculated from the following formula: MDA equivalents (nmol/mL) = $[(A_{532}-A_{600})/\text{MDA } \varepsilon] \times 10^6$, where A_{532} represents the maximum absorbance of the

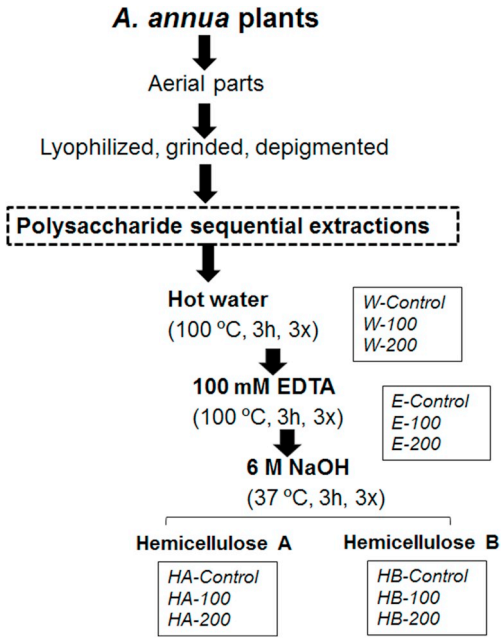

Fig. 8. Scheme for sequential extraction of polysaccharides from aerial parts of *A. annua*. W, fraction obtained with boiling water; E, fraction obtained with 100 mM EDTA; HA, hemicellulose A fraction obtained from 6 M NaOH; HB, hemicellulose B fraction obtained from 6 M NaOH; 100, plants submitted to 100 mM NaCl; 200, plants submitted to 200 mM NaCl.

complex MDA-TBA and A_{600} corrects non-specific interferes. MDA contents were expressed as nmol MDA/mL.

3.3. Sample preparation and polysaccharide extraction

Aerial parts of *A. annua* from each treatment (control, 100 mM NaCl, 200 mM NaCl) were randomly divided in three groups of 3 plants each. Each sample was milled, sieved (32 mesh) and depigmented with absolute ethanol in a Soxhlet apparatus. The resulting material was dried and submitted to sequential extractions using hot water (fractions W), 100 mM EDTA (fractions E) and 6 M NaOH (Fig. 8). After each extraction, the extract was recovered by centrifugation (4700 × *g*), concentrated and treated with ethanol (4 V). Polysaccharides were isolated by centrifugation, treated with absolute ethanol (3x) and dried under vacuum. Extracts obtained using EDTA were dialyzed for 72 h before treatment with ethanol. Alkaline extractions were performed in the presence of $NaBH_4$. Alkaline extracts were neutralized with acetic acid, kept at 4 °C overnight and then, the precipitated fractions were separated by centrifugation and named hemicellulose A (HA). The supernatants were dialyzed for 72 h, concentrated and treated with ethanol (4 V), resulting in hemicellulose B fractions (HB). Final insoluble residues were washed with water, ethanol and acetone and dried under vacuum.

3.4. Monosaccharide composition

Polysaccharides were hydrolyzed with 2 M TFA at 120 °C, for 2 h. Derivatization and GC-MS analysis were performed according to Corrêa-Ferreira et al. [40].

The final insoluble residues and hemicellulose fractions were dissolved in 72% (w/w) H_2SO_4 for 1 h at 0–4 °C, diluted to 8% and kept in boiling water for 15 h. The hydrolyzates were neutralized with $BaCO_3$, the insoluble material was removed and the monosaccharides were reduced and acetylated. Uronic acids content was estimated by colorimetric method [57] using galacturonic or glucuronic acid as standard. Insoluble fractions were hydrolyzed before the colorimetric assay.

3.5. High-performance size-exclusion chromatography (HPSEC)

Isolated polysaccharides were analyzed by HPSEC using a Waters unit coupled to a refractive index (RI), a Wyatt Technology Dawn-F multi-angle laser light scattering (MALLS) detector. Four Waters Ultrahydrogel columns (2000; 500; 250; 120) were connected in series and coupled to the multidetection instrument. A solution of 0.1 M $NaNO_2$ and 0.02% NaN_3 was used as eluent at a flux of 0.6 mL/min. Prior to the analyses, the samples (1.5 mg/mL) were filtered through a 0.22 μm cellulose acetate membrane. The data were collected and analyzed by a Wyatt Technology ASTRA program. All the analyses were carried out at 25 °C.

3.6. Determination of degree of O-methyl esterification

The degree of O-methyl esterification of samples was determined by Fourier transform-infrared (FT-IR) spectroscopy according to Vriesmann et al. [58]. The discs were prepared using KBr and the sample in the proportion 90:10. Spectra were collected at the absorbance mode in the frequency range of 4000–400 cm^{-1} using a Bomem MB-100 spectrophotometer (Hartman & Braun, Canada), at 4 cm^{-1} resolution.

3.7. Nuclear magnetic resonance spectroscopy (NMR)

NMR analyses were performed on a Bruker AVANCE III NMR spectrometer operating at 9.1 T (400 MHz for ^1H), equipped with a 5 mm BBI inverse probe with gradient on the z axis. All spectra were acquired with D_2O solutions (500 μL) using TMSP as reference (δ = 0.00 ppm) or acetone (^1H = 2.22 ppm; ^{13}C = 30.2 ppm), at 70 °C. ^1H NMR analyses were performed with 32 scans, using the standard sequence *zgpr* from Bruker. 2D $^1H/^{13}C$ HSQC (heteronuclear single quantum coherence) were performed using the sequence hsqcetgpsisp2.2 from Bruker, with 16 scans per series of 2048 × 256 W data points with zero filling in F1 (4 K), prior to Fourier transformation. Data procession and integration were performed using the software TOPSPIN version 3.1.

For W and E fractions, from control and saline treatments, relative integration of signals areas of ^1H NMR spectrum was performed. Samples were previously desiccated under vacuum, accurately weighed (10 mg) and dissolved in D_2O (500 μL), containing TMSP-d_4 (0.02%). Samples were transferred to NMR tubes and analyzed at 70 °C, using 32 scans. Presaturation of residual HDO was carried out in spectrum acquisition. Integrated area of signals was relative to TMSP-d_4 area and triplicates of each fraction (W and E) from control and saline treatments were performed.

3.8. Data reduction and multivariate analysis

The spectral window considered was from δ 4.45–6.50. After NMR spectral phase and baseline correction, each spectrum was data-reduced to 1193 regions of equal width (0.001 ppm). All spectra were submitted to Principal Component Analysis (PCA) analyses, using the normalization to total intensity. All analyses were performed using the Software AMIX version 3.8.

3.9. Sulfate content

The presence of sulfate was investigated by the colorimetric 1,9-dimethylmethylene blue (DMB) method [27], using an agarose chemically sulfated, as standard and also by the turbidimetric method [28], which quantifies sulfate as barium sulfate.

3.10. Data analysis

A completely randomized design was used in experiments, with 3 treatments (control, 100 mM NaCl and 200 mM NaCl) and 15 replicates (plants) for each treatment. Nine plants of each treatment were randomly divided in three subgroups for polysaccharide extraction. The results showed for each treatment group are the average of three extractions performed independently. Monosaccharide composition of each sample was done in duplicate. Statistical comparisons between groups were performed using one-way analysis of variance (ANOVA) followed by the Bonferroni's multiple comparison test, using GraphPad Prism, version 8.1.2 for Windows, GraphPad Software, La Jolla California USA. Values of $P < 0.05$ were considered statistically significant.

4. Conclusion

Salt stress negatively affected the growth and biomass accumulation and induced lipid peroxidation in cellular membranes of *A. annua*. Aerial parts were noticeably affected by salt stress, as showed by changes in the monosaccharide composition, yield of polymers and degree of acetylation and methyl esterification. The main changes in cell wall following salt stress were found in the structure of pectins, such as number of side chains of the rhamnogalacturonan, uronic acid content and degree of methyl esterification. According to PCA analysis, the main signals from ^1H NMR that were affected by the treatments correspond to arabinose residues, demonstrating the importance of arabinose for *A. annua* plants under salt stress. Among the hemicelluloses, an increased content of xylose was observed for plants subjected to salt stress. The decrease of xylan substitution suggests a more rigid cell wall in *A. annua* under salt stress, which may help the plant to maintain cellular turgor pressure. No sulfate groups were found in the polysaccharides of *A. annua* submitted to salt stress, indicating that sulfation of cell wall polysaccharides was not a response to salt stress. The main changes of cell wall polysaccharides of *A. annua* were observed in response of 200 mM NaCl, which was the group more affected by salt stress, according to results of physiological parameters (MDA, length, biomass accumulation). As a whole, the results point to a remodeling in the cell wall architecture of *A. annua* in order to tolerate the salt stress condition.

Acknowledgements

The authors thank the Brazilian agencies Coordenação de Aperfeiçoamento de Pessoal de Nível Superior - Brasil (CAPES)-Finance Code 001 and Conselho Nacional de Desenvolvimento Científico e Tecnológico (CNPq) for the financial support and the NMR Center of UFPR. C.L.O.P. is a research member of the CNPq (309159/2018-0).

Appendix A. Supplementary data

Supplementary data to this article can be found online at https://doi.org/10.1016/j.carres.2019.107753.

References

[1] P.J. Weathers, M.A. Elfawal, M.J. Towler, G.K. Acquaah-Mensah, S.M. Rich, Pharmacokinetics of artemisinin delivered by oral consumption of Artemisia annua dried leaves in healthy vs. Plasmodium chabaudi-infected mice, J. Ethnopharmacol. 153 (2014) 732–736, https://doi.org/10.1016/j.jep.2014.03.037.
[2] S.M. Hasheminia, J.J. Sendi, K.T. Jahromi, S. Moharramipour, The effects of Artemisia annua L. and Achillea millefolium L. crude leaf extracts on the toxicity, development, feeding efficiency and chemical activities of small cabbage Pieris rapae L. (Lepidoptera: pieridae), Pestic, Biochem. Physiol. 99 (2011) 244–249, https://doi.org/10.1016/j.pestbp.2010.12.009.
[3] S. Mahajan, N. Tuteja, Cold, salinity and drought stresses: an overview, Arch. Biochem. Biophys. 444 (2005) 139–158, https://doi.org/10.1016/j.abb.2005.10.018.
[4] G. Cherlet, M. Hutchinson, C. Reynolds, J. Hill, J. Sommer, S. von Maltitz (Eds.), World Atlas of Desertification, Publication Office of the European Union, Luxembourg, 2018, https://wad.jrc.ec.europa.eu/.
[5] A. Muszyńska, K. Jarocka, E.U. Kurczynska, Plasma membrane and cell wall

properties of an aspen hybrid (Populus tremula × tremuloides) parenchyma cells under the influence of salt stress, Acta Physiol. Plant. 36 (2014) 1155–1165, https://doi.org/10.1007/s11738-014-1490-3.
[6] T. Aftab, M.M.A. Khan, J.A.T. da Silva, M. Idrees, M. Naeem, Moinuddin, role of salicylic acid in promoting salt stress tolerance and enhanced artemisinin production in Artemisia annua L. J. Plant Growth Regul. 30 (2011) 425–435, https://doi.org/10.1007/s00344-011-9205-0.
[7] Z.H. Qian, K. Gong, L. Zhang, J.B. Lv, F.Y. Jing, Y.Y. Wang, S.B. Guan, G.F. Wang, K.X. Tang, A simple and efficient procedure to enhance artemisinin content in Artemisia annua L. by seeding to salinity stress, Afr. J. Biotechnol. 6 (2007) 1410–1413.
[8] M. Irfan Qureshi, M. Israr, M.Z. Abdin, M. Iqbal, Responses of Artemisia annua L. to lead and salt-induced oxidative stress, Environ. Exp. Bot. 53 (2005) 185–193, https://doi.org/10.1016/j.envexpbot.2004.03.014.
[9] R.B. De Lima, T.B. Dos Santos, L.G.E. Vieira, M. De Lourdes Lúcio Ferrarese, O. Ferrarese-Filho, L. Donatti, M.R.T. Boeger, C.L. De Oliveira Petkowicz, Salt stress alters the cell wall polysaccharides and anatomy of coffee (Coffea arabica L.) leaf cells, Carbohydr. Polym. 112 (2014) 686–694, https://doi.org/10.1016/j.carbpol.2014.06.042.
[10] H. Oliveira, A.S. Barros, I. Delgadillo, M.A. Coimbra, C. Santos, Effects of fungus inoculation and salt stress on physiology and biochemistry of in vitro grapevines: emphasis on sugar composition changes by FT-IR analyses, Environ. Exp. Bot. 65 (2009) 1–10, https://doi.org/10.1016/j.envexpbot.2008.05.003.
[11] R. Tenhaken, Cell wall remodeling under abiotic stress, Front. Plant Sci. 5 (2015) 771, https://doi.org/10.3389/fpls.2014.00771.
[12] P. An, X. Li, Y. Zheng, A. Matsuura, J. Abe, A.E. Eneji, E. Tanimoto, S. Inanaga, Effects of NaCl on root growth and cell wall composition of two soya bean cultivars with contrasting salt tolerance, J. Agron. Crop Sci. 200 (2014) 212–218, https://doi.org/10.1111/jac.12060.
[13] R.S. Aquino, C. Grativol, P.A.S. Mourão, Rising from the sea: correlations between sulfated polysaccharides and salinity in plants, PLoS One 6 (2011) 1–7, https://doi.org/10.1371/journal.pone.0018862.
[14] G. Xie, I.A. Schepetkin, D.W. Siemsen, L.N. Kirpotina, J.A. Wiley, M.T. Quinn, Fractionation and characterization of biologically-active polysaccharides from Artemisia tripartita, Phytochemistry 69 (2008) 1359–1371, https://doi.org/10.1016/j.phytochem.2008.01.009.
[15] N.C. Carpita, D.M. Gibeaut, Structural models of primary cell walls in flowering plants : consistency of molecular structure with the physical properties of the walls during growth, Plant J. 3 (1993) 1–30.
[16] D.J. Cosgrove, Re-constructing our models of cellulose and primary cell wall assembly, Curr. Opin. Plant Biol. 22 (2014) 122–131, https://doi.org/10.1016/j.pbi.2014.11.001.
[17] J.M.C. Silva, N. Dantas-Santos, L.D. Gomes, L.S. Costa, S.L. Cordeiro, M.S.S.P. Costa, N.B. Silva, M.L. Freitas, K.C. Scortecci, E.L. Leite, H.A.O. Rocha, Biological activities of the sulfated polysaccharide from the vascular plant Halodule wrightii, Brazilian J. Pharmacogn. 22 (2011) 94–101, https://doi.org/10.1590/S0102-695X2011005000199.
[18] T.V. Brito, F.C.N. Barros, R.O. Silva, G.J. Dias Júnior, J.S. José, Á.X. Franco, P.M.G. Soares, L.S. Chaves, C.M.W.S. Abreu, R.C.M. de Paula, M.H.L.P. Souza, A.L.P. Freitas, A.L. André, Sulfated polysaccharide from the marine algae Hypnea musciformis inhibits TNBS-induced intestinal damage in rats, Carbohydr. Polym. 151 (2016) 957–964, https://doi.org/10.1016/j.carbpol.2016.06.047.
[19] A.A. Saddhe, M.R. Malvankar, S.B. Karle, K. Kumar, Reactive nitrogen species: paradigms of cellular signaling and regulation of salt stress in plants, Environ. Exp. Bot. 161 (2019) 86–97, https://doi.org/10.1016/j.envexpbot.2018.11.010.
[20] R. Munns, M. Tester, Mechanisms of salinity tolerance, Annu. Rev. Plant Biol. 59 (2008) 651–681, https://doi.org/10.1146/annurev.arplant.59.032607.092911.
[21] R. Munns, Comparative physiology of salt and water stress, Plant Cell Environ. 25 (2002) 239–250, https://doi.org/10.1046/j.0016-8025.2001.00808.x.
[22] H. Gall, F. Philippe, J.-M. Domon, F. Gillet, J. Pelloux, C. Rayon, Cell wall metabolism in response to abiotic stress, Plants 4 (2015) 112–166, https://doi.org/10.3390/plants4010112.
[23] Y. Shavrukov, Salt stress or salt shock: which genes are we studying? J. Exp. Bot. 64 (2013) 119–127.
[24] S.D. Wankhade, A. Sanz, Chronic mild salinity affects source leaves physiology and productivity parameters of rice plants (Oryza sativa L., cv. Taipei 309), Plant Soil 367 (2013) 663–672, https://doi.org/10.1007/s11104-012-1503-1.
[25] R.G. Alscher, N. Erturk, L.S. Heath, Role of superoxide dismutases (SODs) in controlling oxidative stress in plants, J. Exp. Bot. 53 (2002) 1331–1341, https://doi.org/10.1093/jexbot/53.372.1331.
[26] C. Nie, P. Zhu, S. Ma, M. Wang, Y. Hu, Purification, characterization and immunomodulatory activity of polysaccharides from stem lettuce, Carbohydr. Polym. 188 (2018) 236–242, https://doi.org/10.1016/j.carbpol.2018.02.009.
[27] B.O. Enobakhare, D.L. Bader, D. a Lee, Quantification of sulfated glycosaminoglycans in chondrocyte/alginate cultures, by use of 1,9-dimethylmethylene blue, Anal. Biochem. 243 (1996) 189–191, https://doi.org/10.1006/abio.1996.0502.
[28] K. Dodgson, R. Price, A note on the determination of the ester sulphate content of sulphated polysaccharides, Biochem. J. 84 (1962) 106–110, https://doi.org/10.1042/bj0840106.
[29] J. Mustard, S. Renault, Effects of NaCl on water relations and cell wall elasticity and composition of red-osier dogwood (Cornus stolonifera) seedlings, Physiol. Plant. 121 (2004) 265–271, https://doi.org/10.1111/j.1399-3054.2004.00322.x.
[30] C.S. Byrt, R. Munns, R.A. Burton, M. Gilliham, S. Wege, Root cell wall solutions for crop plants in saline soils, Plant Sci. 269 (2018) 47–55.
[31] M.N. Uddin, S. Hanstein, R. Leubner, S. Schubert, Leaf cell-wall components as influenced in the first phase of salt stress in three maize (Zea mays L.) hybrids differing in salt resistance, J. Agron. Crop Sci. 199 (2013) 405–415, https://doi.org/10.1111/jac.12031.
[32] C.M.G.C. Renard, C. Ginies, Comparison of the cell wall composition for flesh and skin from five different plums, Food Chem. 114 (2009) 1042–1049, https://doi.org/10.1016/j.foodchem.2008.10.073.
[33] K.H. Caffall, D. Mohnen, The structure, function, and biosynthesis of plant cell wall pectic polysaccharides, Carbohydr. Res. 344 (2009) 1879–1900, https://doi.org/10.1016/j.carres.2009.05.021.
[34] L. Hocq, J. Pelloux, V. Lefebvre, Connecting homogalacturonan-type pectin remodeling to acid growth, Trends Plant Sci. 22 (2017) 20–29, https://doi.org/10.1016/j.tplants.2016.10.009.
[35] P. Carillo, M.G. Annunziata, G. Pontecorvo, A. Fuggi, P. Woodrow, Salinity stress and salt tolerance, in: A.S (Ed.), Abiotic Stress Plants - Mech. Adapt. InTech, 2011, p. 428 https://doi.org/10.5772/57353.
[36] M.R. Leucci, M.S. Lenucci, G. Piro, G. Dalessandro, Water stress and cell wall polysaccharides in the apical root zone of wheat cultivars varying in drought tolerance, J. Plant Physiol. 165 (2008) 1168–1180, https://doi.org/10.1016/j.jplph.2007.09.006.
[37] V.V. Golovchenko, D.S. Khramova, R.G. Ovodova, A.S. Shashkov, Y.S. Ovodov, Structure of pectic polysaccharides isolated from onion Allium cepa L. using a simulated gastric medium and their effect on intestinal absorption, Food Chem. 134 (2012) 1813–1822, https://doi.org/10.1016/j.foodchem.2012.03.087.
[38] E.G. Shakhmatov, E.V. Udoratina, K.V. Atukmaev, E.N. Makarova, Extraction and structural characteristics of pectic polysaccharides from Abies sibirica L, Carbohydr. Carbohydr. Poly. 123 (2015) 228–236, https://doi.org/10.1016/j.carbpol.2015.01.041.
[39] Z. Kostalova, Z. Hromádková, A. Ebringerová, Structural diversity of pectins isolated from the Styrian oil-pumpkin (Cucurbita pepo var. styriaca) fruit, Carbohydr. Polym. 93 (2013) 163–171, https://doi.org/10.1016/j.carbpol.2012.05.017.
[40] M.L. Corrêa-Ferreira, D.M. Ferreira, J.L. Dallazen, A.M.S. Silva, M.F. de P. Werner, C.L. de O. Petkowicz, Gastroprotective effects and structural characterization of a pectic fraction isolated from Artemisia campestris subsp maritima, Int. J. Biol. Macromol. 107 (2018) 2395–2403, https://doi.org/10.1016/j.ijbiomac.2017.10.127.
[41] D. Wefers, C.E. Tyl, M. Bunzel, Novel arabinan and galactan oligosaccharides from dicotyledonous plants, Front. Chem. 2 (2014) 1–9, https://doi.org/10.3389/fchem.2014.00100.
[42] F. Sénéchal, C. Wattier, C. Rustérucci, J. Pelloux, Homogalacturonan-modifying enzymes: structure, expression, and roles in plants, J. Exp. Bot. 65 (2014) 5125–5160, https://doi.org/10.1093/jxb/eru272.
[43] M.L. Corrêa-Ferreira, G.R. Noleto, C.L. Oliveira Petkowicz, Artemisia absinthium and Artemisia vulgaris: a comparative study of infusion polysaccharides, Carbohydr. Polym. 102 (2014) 738–745, https://doi.org/10.1016/j.carbpol.2013.10.096.
[44] H.-J. Gao, H.-Y. Yang, J.-P. Bai, X.-Y. Liang, Y. Lou, J.-L. Zhang, D. Wang, J.-L. Zhang, S.-Q. Niu, Y.-L. Chen, Ultrastructural and physiological responses of potato (Solanum tuberosum L.) plantlets to gradient saline stress, Front. Plant Sci. 5 (2014) 787, https://doi.org/10.3389/fpls.2014.00787.
[45] Y.G. Yin, Y. Kobayashi, A. Sanuki, S. Kondo, N. Fukuda, H. Ezura, S. Sugaya, C. Matsukura, Salinity induces carbohydrate accumulation and sugar-regulated starch biosynthetic genes in tomato (Solanum lycopersicum L. cv. 'Micro-Tom') fruits in an ABA-and osmotic stress-independent manner, J. Exp. Bot. 61 (2010) 563–574, https://doi.org/10.1093/jxb/erp333.
[46] H. Greenway, R. Munns, Mechanisms of salt tolerance in nonhalophytes, Annu. Rev. Plant Physiol. 31 (1980) 149–190.
[47] M. Busse-Wicher, T.C.F. Gomes, T. Tryfona, N. Nikolovski, K. Stott, N.J. Grantham, D.N. Bolam, M.S. Skaf, P. Dupree, The pattern of xylan acetylation suggests xylan may interact with cellulose microfibrils as a twofold helical screw in the secondary plant cell wall of Arabidopsis thaliana, Plant J. 79 (2014) 492–506, https://doi.org/10.1111/tpj.12575.
[48] Y. Guan, B. Zhang, X.M. Qi, F. Peng, C.L. Yao, R.C. Sun, Fractionation of bamboo hemicelluloses by graded saturated ammonium sulphate, Carbohydr. Polym. 129 (2015) 201–207, https://doi.org/10.1016/j.carbpol.2015.04.042.
[49] P. Peng, F. Peng, J. Bian, F. Xu, R.C. Sun, J.F. Kennedy, Isolation and structural characterization of hemicelluloses from the bamboo species Phyllostachys incarnata Wen, Carbohydr. Polym. 86 (2011) 883–890, https://doi.org/10.1016/j.carbpol.2011.05.038.
[50] Q. Guo, S.W. Cui, Q. Wang, X. Hu, Y. Wu, J. Kang, R. Yada, Structure characterization of high molecular weight heteropolysaccharide isolated from Artemisia sphaerocephala Krasch seed, Carbohydr. Polym. 86 (2011) 742–746, https://doi.org/10.1016/j.carbpol.2011.05.018.
[51] N.C. Carpita, Structure and biogenesis of the cell walls of grasses, Annu. Rev. Plant Physiol. Plant Mol. Biol. 47 (1996) 445–476, https://doi.org/10.1146/annurev.arplant.47.1.445.
[52] A. Gribaa, F. Dardelle, A. Lehner, C. Rihouey, C. Burel, A. Ferchichi, A. Driouich, J.C. Mollet, Effect of water deficit on the cell wall of the date palm (Phoenix dactylifera "Deglet nour", Arecales) fruit during development, Plant Cell Environ. 36 (2013) 1056–1070, https://doi.org/10.1111/pce.12042.
[53] S.E. de Araújo Neto, J.M.A. de Azevedo, R. de O. Galvão, E.B. de L. Oliveira, R.L.F. Ferreira, Produção de muda orgânica de pimentão com diferentes substratos, Ciência Rural. 39 (2009) 1408–1413, https://doi.org/10.1590/s0103-84782009005000099.
[54] J.V. Fontenelli, T.J.A. da Silva, E.M. Bonfim-Silva, H.H.F. Sousa, Methods of soil moisture maintenance for production of sunflower under controlled conditions, Aust. J. Crop. Sci. 11 (2017) 580–584.
[55] H. Nivison, L. Fish, A. Jagendorf, Translation by isolated pea chloroplasts, in:

A. Weissbach, H. Weissbach (Eds.), Methods Plant Mol. Biol. 1988, pp. 159–172 London.
[56] I. Cakmak, W.J. Horst, Effect of aluminium on lipid peroxidation, superoxide dismutase, catalase, and peroxidase activities in root tips of soybean (Glycine max), Physiol. Plant. 83 (1991) 463–468, https://doi.org/10.1111/j.1399-3054.1991.tb00121.x.
[57] N. Blumenkrantz, G. Asboe-Hansen, New method for quantitative determination of uronic acids, Anal. Biochem. 54 (1973) 484–489, https://doi.org/10.1016/0003-2697(73)90377-1.
[58] L.C. Vriesmann, C.L. de O. Petkowicz, Polysaccharides from the pulp of cupuassu (Theobroma grandiflorum): structural characterization of a pectic fraction, Carbohydr. Polym. 77 (2009) 72–79, https://doi.org/10.1016/j.carbpol.2008.12.007.